Mean-Square Radius of Gyration of Oligo- and Poly(α-methylstyrene)s in Dilute Solution

Masashi Osa,† Takenao Yoshizaki, and Hiromi Yamakawa*

Department of Polymer Chemistry, Kyoto University, Kyoto 606-8501, Japan

Received February 28, 2000; Revised Manuscript Received April 11, 2000

ABSTRACT: The mean-square radius of gyration $\langle S^2 \rangle$ was determined from small-angle X-ray and light scattering measurements for 20 samples of atactic oligo- and poly(α-methylstyrene)s (a-PαMS), each with the fraction of racemic diads $f_r = 0.72$, in the range of weight-average molecular weight from 6.48×10^2 (pentamer) to 3.22×10^6 in cyclohexane at 30.5 °C (Θ). The ratio $\langle S^2 \rangle / x_w$ as a function of the weight-average degree of polymerization x_w first increases steeply for $x_w \lesssim 20$, then passes through a flat hump at $x_w \simeq 40$, and finally approaches its asymptotic value for $x_w \gtrsim 1 \times 10^3$. On the basis of the helical wormlike (HW) chain model the HW model parameters are $\lambda^{-1}\kappa_0 = 3.0$, $\lambda^{-1}\tau_0 = 0.9$, $\lambda^{-1} = 46.8$ Å, and $M_L = 39.8$ Å^{-1}, where κ_0 and τ_0 are the differential-geometrical curvature and tortion, respectively, of the characteristic helix of the HW chain taken at the minimum zero of its elastic energy, λ^{-1} is the stiffness parameter, and M_L is the shift factor defined as the molecular weight per unit contour length of the chain. The local chain conformations of a-PαMS are discussed in detail on the basis of the above values of the model parameters and compared with those of atactic polystyrene ($f_r = 0.59$), atactic poly(methyl methacrylate) (a-PMMA) ($f_r = 0.79$), and isotactic PMMA ($f_r \simeq 0.01$) previously studied. It is then concluded that the a-PαMS chain tends to retain large and clearly distinguishable helical portions in dilute solution like the a-PMMA chain, as was expected from their chemical structures, although the helical nature of the former is somewhat weaker. To illustrate the situation, pictures are given of representative instantaneous contours of HW Monte Carlo chains for the above four polymers.

Introduction

During the past decade a series of experimental studies[1] of dilute solution behavior of some flexible polymers and their oligomers have been reported in the unperturbed Θ state on the basis of the helical wormlike (HW) chain model[2,3] to obtain information about their chain stiffness and local chain conformations. Among the polymers studied so far, atactic poly(methyl methacrylate) (a-PMMA) with the fraction of racemic diads $f_r = 0.79$ has been shown to have the largest chain stiffness and the strongest helical nature.[2,4] It turns out that the a-PMMA chain tends to retain rather large and clearly distinguishable helical portions in dilute solution. Such a remarkable feature of this chain may be regarded as arising from the inequality of the two successive skeletal bond angles and the predominance of the trans−trans conformation for its racemic diads.[2,5]

Atactic poly(α-methylstyrene) (a-PαMS) is a disubstituted asymmetric polymer and belongs to the same category as a-PMMA, and therefore, the two chains with large f_r may be expected to be similar in their dilute solution behavior. The result of analysis[6] of the data for the rotational isomeric state model[7] is consistent with this expectation. On the other hand, there have been a number of experimental investigations[8−12] of a-PαMS. Unfortunately, however, all have used samples with rather large molecular weight M ($\gtrsim 5 \times 10^4$) and the data obtained were analyzed on the basis of the Gaussian chain model[13] or the Kratky−Porod (KP) wormlike chain model,[2,14] so that they do not give any information about the local chain conformations of a-PαMS in dilute solution. Under these circumstances, it is desirable to pursue further an experimental study of dilute solution properties of a-PαMS in the same spirit as in the previous studies.[1] In this work, we make a start in this study by determining the mean-square radius of gyration $\langle S^2 \rangle$ from light and small-angle X-ray scattering measurements for a-PαMS in a Θ solvent, cyclohexane, over a wide range of M, including the oligomers of very low M.

It has been previously shown that for a polymer with strong helical nature such as a-PMMA, the ratio of $\langle S^2 \rangle$ to the degree of polymerization x as a function of x exhibits a maximum.[2,4] Thus the behavior of the ratio for a-PαMS may be expected to be similar if its helical nature is as strong as that of a-PMMA. The primary object of this paper is to confirm this experimentally.

It is pertinent to make some remarks here on the a-PαMS samples used in this work. As often mentioned in the previous studies,[1] the dilute solution behavior of mono- and disubstituted asymmetric polymers, including a-PαMS, depends remarkably on the stereochemical composition as specified by f_r, so that samples with fixed f_r should be used in this work. Furthermore, it is suitable for the present purpose to use samples whose f_r are as large as that for a-PMMA previously studied.[4] Such a set of a-PαMS samples with $f_r = 0.72 \pm 0.01$ have been successfully prepared by anionic polymerization,[15] giving particular attention to the polymerization temperature and the initial monomer concentration with the help of the results reported by Elgert and coworkers.[16,17]

Experimental Section

Materials. All the original a-PαMS samples were prepared by living anionic polymerization,[15] except the sample named 20538-2, which is a commercial one from Polymer Laboratories Ltd. The polymerization was carried out in tetrahydrofuran with *sec*-butyllithium as an initiator, giving particular attention to the polymerization conditions. Elgert and Seiler[16]

† Research Fellow of the Japan Society for the Promotion of Science.

10.1021/ma000353i CCC: $19.00
Published on Web 06/08/2000

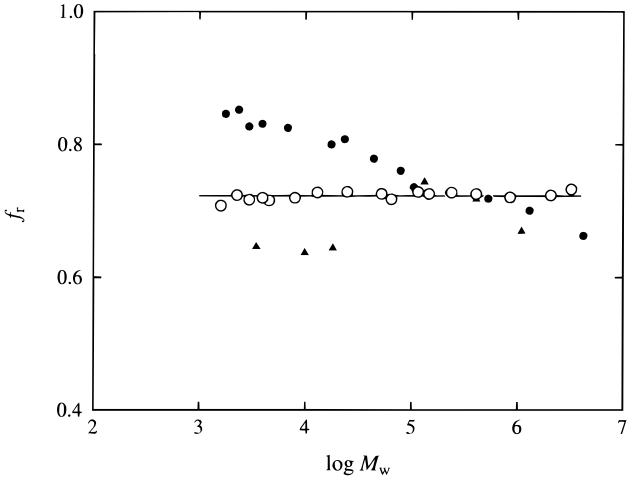

Figure 1. Plots of f_r against log M_w for a-PαMS: (○) present samples; (●) those prepared by Elgert and Seiler;[16] (▲) commercial ones (Polymer Laboratory Ltd.).

clearly showed that f_r of an a-PαMS sample polymerized at constant polymerization temperature T_p increases with decreasing M, as shown in Figure 1, where f_r values are plotted against the logarithm of the weight-average molecular weight M_w for their samples polymerized at −75 °C (filled circles). Subsequently, Wicke and Elgert[17] showed that f_r of a polymerized sample with a given M increases with increasing T_p and that it may also be somewhat dependent on the initial monomer concentration $[M]_0$. Considering these facts, we changed T_p from −70 to −40 °C with increasing M with $[M]_0$ kept at ca. 0.6 mol/L so that f_r was constant for all the polymerized samples.

The polymerization was terminated by adding methanol after the reaction proceeded for ca. 1 min for $M \lesssim 1 \times 10^3$, ca. 5 min for $1 \times 10^3 \lesssim M \lesssim 5 \times 10^4$, ca. 20 min for $5 \times 10^4 \lesssim M \lesssim 5 \times 10^5$, and ca. 2 h for $M \gtrsim 5 \times 10^5$. The initiating chain end of each original a-PαMS sample so obtained is a *sec*-butyl group, and the other end is a hydrogen atom. We note that although detailed information about the polymerization of the commercial sample could not be obtained, its initiating and terminating chain ends may be considered to be an *n*-butyl group and a hydrogen atom, respectively.

The original synthesized and commercial samples were separated into fractions by preparative gel permeation chromatography (GPC) for the test samples with $M \lesssim 2 \times 10^3$ and by fractional precipitation using benzene as a solvent and methanol as a precipitant for those with $M \gtrsim 2 \times 10^3$. In the first column of Table 1 are given the codes of all the samples used in this work. We note that the three groups of the samples OAMS5−OAMS13, OAMS19 and OAMS25, and OAMS33 and OAMS38 are fractions from three original samples, respectively, and the sample AMS40 is a fraction from the commercial sample 20538-2. The test samples with $M \lesssim 1 \times 10^3$ were dissolved in benzene, then filtered through a Teflon membrane of pore size 0.45 μm, and finally dried in a vacuum at 30−40 °C for 15−30 days. The test samples with $M \gtrsim 1 \times 10^3$ were freeze-dried from their benzene solutions after filtration through a membrane of the same kind.

The values of f_r determined from ^{1}H NMR spectra for the test samples[15] are given in the fifth column of Table 1. Although f_r of the samples OAMS5−OAMS10 could not be determined because of the complexity of their ^{1}H NMR spectra, they may be regarded as having almost the same value (∼0.71) of f_r as OAMS13, since the six samples OAMS5−OAMS13 are fractions from one original sample, as mentioned above. In this connection, we note that the value of f_r of the trimer sample, which was also separated from the same original sample but not used in this work, was determined to be 0.73.[15] In Figure 1 are also plotted the values of f_r of the samples OAMS13−AMS320 (unfilled circles). The values of M_w for these and other test samples (in the second column of Table 1) are mentioned

Table 1. Values of M_w, x_w, M_w/M_n, and f_r for Atactic Oligo- and Poly(α-methylstyrene)s

sample	M_w	x_w	M_w/M_n	f_r
OAMS5	6.48×10^2	5	<1.01	
OAMS6	7.66×10^2	6	<1.01	
OAMS7	8.84×10^2	7	<1.01	
OAMS8	1.04×10^3	8.29	1.01	
OAMS10	1.27×10^3	10.3	1.01	
OAMS13	1.60×10^3	13.1	1.02	0.71
OAMS19	2.27×10^3	18.7	1.07	0.72
OAMS25	2.96×10^3	24.6	1.06	0.72
OAMS33	3.95×10^3	33.0	1.04	0.72
OAMS38	4.57×10^3	38.2	1.07	0.72
OAMS67	7.97×10^3	67.1	1.04	0.72
AMS1	1.30×10^4	109	1.02	0.73
AMS2	2.48×10^4	209	1.02	0.73
AMS5	5.22×10^4	442	1.02	0.73
AMS6	6.46×10^4	547	1.03	0.72
AMS24	2.38×10^5	2010	1.05	0.73
AMS40[a]	4.07×10^5	3450	1.02	0.73
AMS80	8.50×10^5	7200	1.05	0.72
AMS200	2.06×10^6	17400	1.05	0.72
AMS320	3.22×10^6	27300		0.73

[a] Separated from the commercial sample 20538-2.

in the next (Results) section. It is seen from Figure 1 and Table 1 that all the samples have almost the same value 0.72 ± 0.01 of f_r independent of M_w. In the figure, the filled triangles represent the values of f_r of six commercial samples from Polymer Laboratories Ltd., including the sample 20538-2 mentioned above, which are seen not to be suitable for our present purpose.

The solvent cyclohexane used for light scattering (LS) and small-angle X-ray scattering (SAXS) measurements was purified according to a standard procedure.

Light Scattering. LS measurements were carried out to determine M_w for all the samples with $M_w \gtrsim 1 \times 10^3$, the Θ temperature of a-PαMS solutions in cyclohexane, and $\langle S^2 \rangle$ for the samples with $M_w \gtrsim 2 \times 10^5$. M_w was determined in cyclohexane at Θ. For the determination of Θ, the second virial coefficient A_2 was measured for the three samples AMS40, AMS200, and AMS320 at several temperatures ranging from 26.0 to 35.0 °C.

A Fica 50 light-scattering photometer was used for all the measurements with vertically polarized incident light of wavelength 436 nm. For a calibration of the apparatus, the intensity of light scattered from pure benzene was measured at 25.0 °C at a scattering angle of 90°, where the Rayleigh ratio $R_{Uu}(90°)$ of pure benzene was taken as 46.5×10^{-6} cm^{-1}.[18] The depolarization ratio ρ_u of pure benzene at 25.0 °C was determined to be 0.41 ± 0.01. Scattered intensities were measured at five or six different concentrations and at scattering angles ranging from 22.5 to 150°. The data obtained were treated by using the Berry square-root plot.[19] In the determination of A_2, the Bawn plot[20] was also used. For the samples with $M_w \gtrsim 2 \times 10^3$, corrections for the optical anisotropy were unnecessary since the degree of depolarization was negligibly small, but for $1 \times 10^3 \lesssim M_w \lesssim 2 \times 10^3$, measurements with unpolarized incident light were also carried out to make those necessary corrections.

The most concentrated solution of each sample was prepared gravimetrically and made homogeneous by continuous stirring at 50 °C for 7 days. It was optically purified by filtration through a Teflon membrane of pore size 0.45 or 0.10 μm. The solutions of lower concentrations were obtained by successive dilution. The weight concentrations of the test solutions were converted to the polymer mass concentrations c by the use of the densities of the respective solutions calculated with the partial specific volumes v_2 of the samples and with the density ρ_0 of the solvent cyclohexane. The quantities v_2 and ρ_0 were measured with a pycnometer of the Lipkin−Davison type having the volume of 10 cm^3. The values of v_2 so determined in cyclohexane at Θ are 0.960, 0.958, 0.939, 0.938, 0.916, 0.913, 0.905, 0.892, 0.891, 0.890, 0.889, and 0.887 cm^3/g for the

samples OAMS5−AMS1, respectively, and 0.885 cm^3/g for the samples with $M_w \gtrsim 2 \times 10^4$ independently of M_w. The value of ρ_0 of cyclohexane at Θ is 0.7683 g/cm^3. We note that ν_2 is independent of temperature in the range from 25.0 to 35.0 °C for $M_w \gtrsim 2 \times 10^4$.

The refractive index increment $\partial n/\partial c$ was measured at wavelength of 436 nm by the use of a Shimadzu differential refractometer. The values of $\partial n/\partial c$ determined in cyclohexane at Θ are 0.182_1, 0.187_0, 0.188_0, 0.194_7, 0.194_7, 0.196_9, 0.198_1, 0.201_2, 0.201_5, 0.200_7, 0.200_5, and 0.201_9 cm^3/g for the samples OAMS8−AMS6, respectively, and 0.203_7 cm^3/g for the samples with $M_w \gtrsim 1 \times 10^5$ independently of M_w. In contrast to the case of ν_2 above, $\partial n/\partial c$ of the samples with $M_w \gtrsim 1 \times 10^5$ was found to depend on temperature T (in °C) and may be given empirically by

$$\partial n/\partial c = 0.190_4 + 4.3_6 \times 10^{-4} T \qquad (1)$$

in the range from 25.0 to 35.0 °C.

For the refractive index n_0 of cyclohexane at Θ at wavelength of 436 nm, we use the value 1.429_8 calculated from an interpolation formula[21] as a function of T.

Small-Angle X-ray Scattering. SAXS measurements were carried out for 15 samples with $M_w \lesssim 7 \times 10^4$ in cyclohexane at Θ by the use of an Anton Paar Kratky U-slit camera with an incident X-ray of wavelength 1.54 Å (Cu Kα line). The apparatus system and the methods of data acquisition and analysis are the same as those described in a previous paper.[22]

The measurements were performed for four or five solutions of different concentrations for each polymer sample and for the solvent at scattering angles ranging from 1×10^{-3} rad to a value at which the scattered intensity was negligibly small. Corrections for the stability of the X-ray source and the detector electronics were made by measuring the intensity scattered from Lupolene (a platelet of polyethylene) used as a working standard before and after each measurement for a given sample solution and the solvent. The effect of absorption of X-rays by a given solution or the solvent was also corrected by measuring the intensity scattered from Lupolene with insertion of the solution or solvent between the X-ray source and Lupolene. The degree of absorption increased linearly with increasing solute concentration.

The excess reduced scattered intensity $\Delta I_R(k)$ as a function of the scattering vector k was determined from the observed (smeared) excess reduced intensity by the modified Glatter desmearing method, which consists of expressing the true scattering function in terms of cubic B-spline functions, as described before.[22] Here, k is given by

$$k = (4\pi/\lambda_0) \sin(\theta/2) \qquad (2)$$

with λ_0 the wavelength of the incident X-ray and θ the scattering angle. Then the data for $\Delta I_R(k)$ were analyzed by using the Berry square-root plot[19] to evaluate the apparent mean-square radius of gyration $\langle S^2 \rangle_s$.

The test solutions of each sample were prepared in the same manner as that in the case of LS measurements.

Results

Molecular Weights and Their Distributions. The values of M_w, the weight-average degree of polymerization x_w, and the ratio of M_w to the number-average molecular weight M_n for the a-PαMS samples used for the determination of $\langle S^2 \rangle$ are given in the second through fourth columns of Table 1, respectively. The three oligomer samples OAMS5, OAMS6, and OAMS7 were confirmed by analytical GPC to be almost monodisperse ($M_w/M_n < 1.01$) and also to be the pentamer, hexamer, and heptamer, respectively. For the other samples OAMS8−AMS320, the values of M_w were determined from LS measurements in cyclohexane at Θ. The values of M_w/M_n for the samples OAMS8−AMS200 were also determined by analytical GPC. It is seen from the table that all the samples except AMS320 are very narrow in molecular weight distribution. Although the value of M_w/M_n for the sample AMS320 could not be determined with high accuracy because of the lack of the GPC calibration curve in the necessary range, its molecular weight distribution may be considered to be as narrow as that of the other samples.

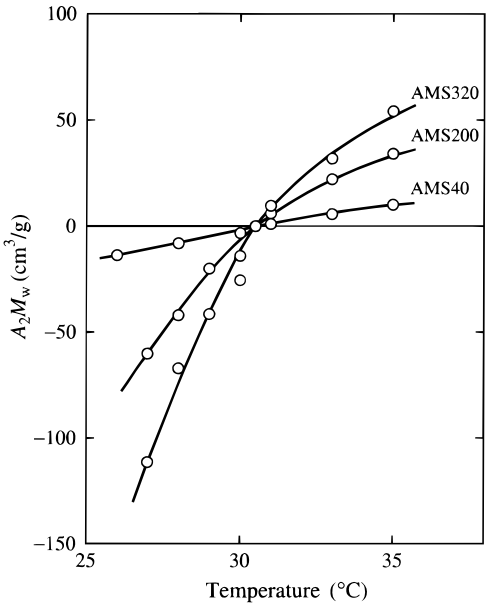

Figure 2. Plots of A_2M_w against temperature for the indicated a-PαMS samples in cyclohexane.

As already mentioned in the Experimental Section, all the samples, including OAMS5−OAMS10, have almost the same value 0.72 ± 0.01 of f_r. However, their stereochemical compositions require a remark. The diad distribution in a chain was shown not to be Bernoullian, and therefore, the fractions of stereoisomeric sequences in the triad rather than f_r must be used for a complete specification of the stereochemical composition.[15] However, those fractions were also found to be almost independent of M_w, so that we simply specify the composition of our a-PαMS only by f_r as in the previous paper.[15]

Θ Temperature. Figure 2 shows plots of A_2M_w against temperature for the three samples AMS40, AMS200, and AMS320 in cyclohexane. It is seen from the figure that A_2 vanishes at almost the same temperature independent of M_w, leading to the conclusion that the Θ temperature is 30.5 °C for solutions of the a-PαMS with $f_r = 0.72$ in cyclohexane. We note that the M_w for these three samples are so large that the effect of chain ends on A_2 is negligibly small (see Chapter 8 of ref 2). This value of the Θ temperature is somewhat lower than the literature values 34.5 °C determined by Kato et al.[23] for a-PαMS with $f_r \simeq 0.63$ and 34.9 °C by Tsunashima[10] for a-PαMS with $f_r \simeq 0.68$. Cowie and Bywater[24] reported that the Θ temperature increased from 32.3 to 36.8 °C with decreasing f_r from 0.95 to 0.67, although the samples used by them were quite polydisperse and their molecular weights were not sufficiently high to neglect the possible effect of chain ends on A_2. Our somewhat low value of Θ may then be regarded as arising mainly from our rather large f_r. Further, we note that Lindner et al.[25] determined Θ to be 36.2 °C for a-PαMS with $f_r \simeq 0.74$, where the determination was made so that the Houwink−Mark−Sakurada exponent

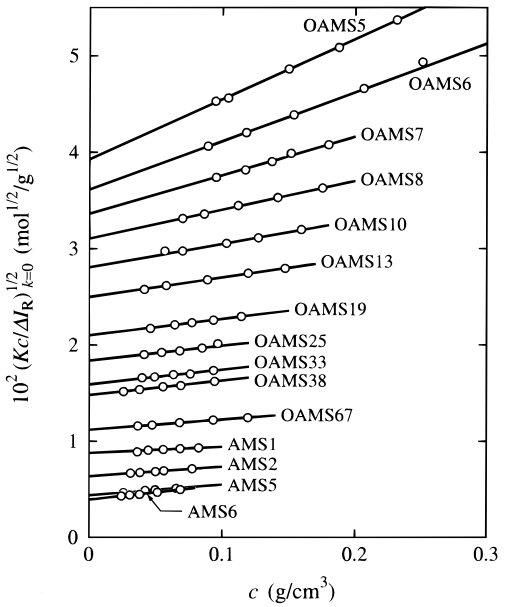

Figure 3. Plots of $(Kc/\Delta I_R)_{k=0}^{1/2}$ against c for the indicated a-PαMS samples in cyclohexane at 30.5 °C.

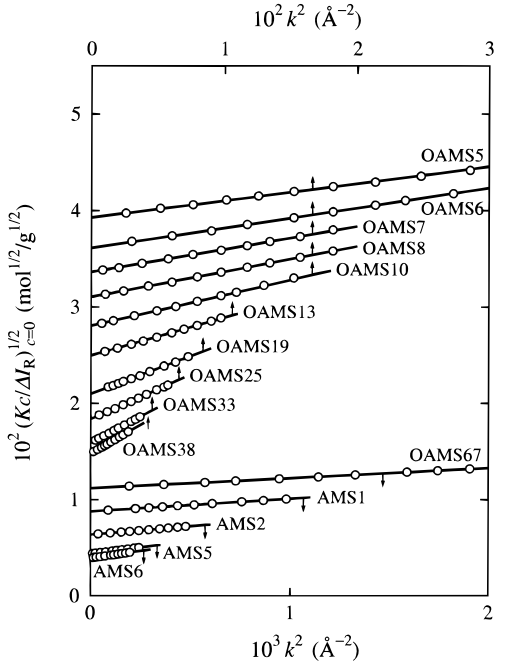

Figure 4. Plots of $(Kc/\Delta I_R)_{c=0}^{1/2}$ against k^2 for the indicated a-PαMS samples in cyclohexane at 30.5 °C.

became 0.5 in the range of $5 \times 10^4 \lesssim M_w \lesssim 1 \times 10^6$. For polymers with strong helical nature, for which the exponent in this range is appreciably smaller than 0.5 at Θ (see Chapter 6 of ref 2), such a procedure is less reliable than the direct one above.

Mean-Square Radii of Gyration $\langle S^2\rangle_s$ and $\langle S^2\rangle$. The values of $(c/\Delta I_R)_{k=0}^{1/2}$ and $(c/\Delta I_R)_{c=0}^{1/2}$ for the samples OAMS5−AMS6 ($6.48 \times 10^2 \lesssim M_w \lesssim 6.46 \times 10^4$) in cyclohexane at 30.5 °C (Θ) were determined by extrapolation to zero angle and zero concentration, respectively, from the SAXS data for $(c/\Delta I_R)^{1/2}$ obtained at finite scattering angles and concentrations. Figures 3 and 4 show plots of $(Kc/\Delta I_R)_{k=0}^{1/2}$ against c and those of $(Kc/\Delta I_R)_{c=0}^{1/2}$ against k^2, respectively, where K is the optical constant which depends on the SAXS apparatus (and also the cell) used. We used a new SAXS cell in the present study, and therefore, the value of K for this cell is different from those for the cells used in the previous studies. Thus, in the figures, we have chosen its value for each sample so that the value of the common intercept $(Kc/\Delta I_R)_{c=0,k=0}^{1/2}$ at $c = 0$ and $k = 0$ is consistent with the value of M_w in Table 1 determined from LS measurements or by analytical GPC, for convenience. Note that they may be related to each other by

$$(Kc/\Delta I_R)_{c=0,k=0}^{1/2} = M_w^{-1/2} \tag{3}$$

and also that the choice of K does not affect the determination of $\langle S^2\rangle$.

In Figure 3, the straight line fitted to the data points for each sample for $M_w < 10^5$ has definitely a positive slope, indicating that A_2 does not vanish for a-PαMS oligomers even in the unperturbed Θ state, i.e., at the Θ temperature at which A_2 vanishes for large M_w ($\gtrsim 10^5$). The same behavior has also been found for the SAXS data for the atactic polystyrene (a-PS)[22] and a- and isotactic (i-) PMMA[4,26] oligomers at the respective Θ temperatures. As noted in a previous LS study of A_2 for a-PMMA,[27] SAXS data are not sufficiently accurate to arrive at a quantitative conclusion on this point, so that we do not further discuss the results.

In Figure 4, the data points for each sample also follow the indicated straight line in the range of k^2 displayed, thereby permitting an accurate determination of the apparent mean-square radius of gyration $\langle S^2\rangle_s$ from the ratio of its slope to its intercept.[22] The values of $\langle S^2\rangle_s^{1/2}$ so determined are listed in the second and fifth columns of Table 2. As always done in the previous papers,[2,4,22,26] these values of $\langle S^2\rangle_s$ may be converted to those of $\langle S^2\rangle$ itself of the chain contour by the relation[2,22]

$$\langle S^2\rangle_s = \langle S^2\rangle + S_c^2 \tag{4}$$

where we note that the latter should be compared with the HW theoretical expression derived for the chain contour and that this relation has been derived for a continuous model chain having a uniform circular cross section of diameter d with S_c being the radius of gyration of the cross section.[22]

In this work, we make the above correction by adopting the value 10.7 Å^2 of S_c^2 calculated from the relation $S_c^2 = d^2/8 = \nu_2 M_L/2\pi N_A$ with N_A the Avogadro constant and M_L the shift factor, the molecular weight per unit contour length of the continuous chain. Here, we have used the value 0.88_5 cm^3/g of ν_2 for the a-PαMS samples with very large M_w and the value 45.7 Å^{-1} of M_L corresponding to the chain fully extended to the all-trans conformation as in the cases of a- and i-PMMAs.[4,26] The results for $\langle S^2\rangle^{1/2}$ so obtained are given in the third and sixth columns of Table 2. For a-PαMS, $\langle S^2\rangle_s$ is seen to become equal to $\langle S^2\rangle$ for $M_w \gtrsim 10^4$.

Table 2. Results of SAXS Measurements for Atactic Oligo- and Poly(α-methylstyrene)s in Cyclohexane at 30.5 °C

sample	$\langle S^2\rangle_s^{1/2}$, Å	$\langle S^2\rangle^{1/2}$, Å	sample	$\langle S^2\rangle_s^{1/2}$, Å	$\langle S^2\rangle^{1/2}$, Å
OAMS5	5.1_7	4.0_1	OAMS33	$16._6$	$16._2$
OAMS6	5.8_7	4.8_7	OAMS38	$17._9$	$17._6$
OAMS7	6.4_9	5.6_1	OAMS67	$23._7$	$23._4$
OAMS8	7.1_1	6.3_2	AMS1	$30._2$	$30._0$
OAMS10	8.2_4	7.5_6	AMS2	$41._1$	$40._9$
OAMS13	9.7_3	9.1_6	AMS5	$60._3$	$60._2$
OAMS19	$12._2$	$11._8$	AMS6	$66._7$	$66._7$
OAMS25	$14._2$	$13._8$			

Table 3. Results of LS Measurements for Atactic Poly(α-methylstyrene) in Cyclohexane at 30.5 °C

sample	$10^{-2}\langle S^2\rangle^{1/2}$, Å	sample	$10^{-2}\langle S^2\rangle^{1/2}$, Å
AMS24	1.2_9	AMS200	3.7_6
AMS40	1.6_6	AMS320	4.6_5
AMS80	2.4_1		

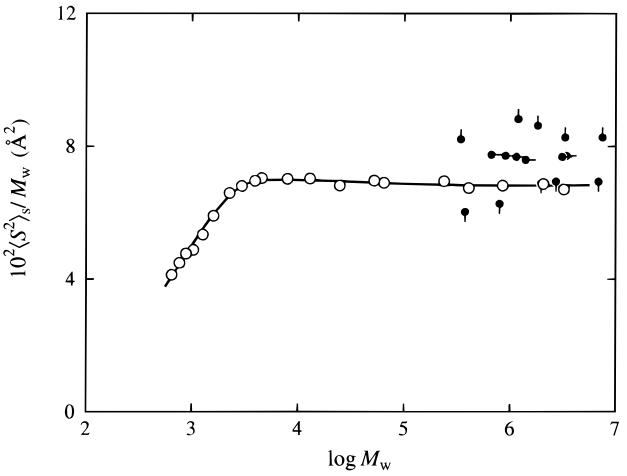

Figure 5. Molecular weight dependence of $\langle S^2\rangle_s/M_w$ for a-PαMS in cyclohexane: (○) present SAXS and LS data at 30.5 °C; (filled circle with pip up) LS data at 34.5 °C by Kato et al.;[8] (filled circle with pip down) LS data at 34.9 °C by Tsunashima;[10] (filled circle with pip right) LS data at 36.2 °C by Li et al.[12] The solid curve connects smoothly the present data points.

Table 3 summarizes the results obtained for $\langle S^2\rangle$ from LS measurements for the samples with $M_w \gtrsim 2 \times 10^5$ in cyclohexane at 30.5 °C (Θ).

Molecular Weight Dependence of $\langle S^2\rangle_s/M_w$. The ratio $\langle S^2\rangle_s/M_w$ is plotted against log M_w in Figure 5 with the present data for a-PαMS with $f_r = 0.72$ in cyclohexane at 30.5 °C (Θ) (unfilled circles). As mentioned in the last subsection, the contribution of S_c^2 to $\langle S^2\rangle_s$ becomes negligibly small (i.e., $\langle S^2\rangle_s = \langle S^2\rangle$) for $M_w \gtrsim 10^4$, and therefore the values from SAXS (for $M_w \lesssim 7 \times 10^4$) are smoothly jointed to those from LS (for $M_w \gtrsim 2 \times 10^5$), the latter being almost independent of M_w as in the cases of the other polymers previously studied. In the figure, the solid curve connects smoothly the data points. As M_w is increased, $\langle S^2\rangle_s/M_w$ first increases steeply for $M_w \lesssim 2 \times 10^3$, then passes through a flat hump at $M_w \simeq 4 \times 10^3$, and finally approaches its asymptotic value for $M_w \gtrsim 10^5$.

For comparison, literature data for a-PαMS in cyclohexane are also plotted in the figure (filled circles) for the samples with $f_r \simeq 0.63$ at 34.5 °C by Kato et al.[8] (with pip up), those with $f_r \simeq 0.68$ at 34.9 °C by Tsunashima[10] (with pip down), and those with $f_r \simeq 0.74$ at 36.2 °C by Li et al.[12] (with pip right). The values of $\langle S^2\rangle$ by Tsunashima agree with ours within experimental error for $M_w \gtrsim 10^6$, while both the values by Kato et al. and by Li et al. are appreciably larger than ours. We note that the difference between our and Kato et al.'s values may probably be mainly due to that in f_r or in helical nature (see also the next section) and that the values by Li et al. may be considered to be overestimated because of the use of the Zimm plot (and also of their somewhat high Θ temperature).

Discussion

HW Model Parameters. Now we determine the model parameters of a-PαMS as the HW chain from a comparison of the experimental values of $\langle S^2\rangle$ given in the last section with the corresponding HW theoretical values. The theoretical $\langle S^2\rangle$ may be expressed in terms of the four basic model parameters: the differential-geometrical curvature κ_0 and torsion τ_0 of the characteristic helix of the HW chain taken at the minimum zero of its elastic energy, the static stiffness parameter λ^{-1}, and the shift factor M_L.[2]

For the HW chain of total contour length L without excluded volume, $\langle S^2\rangle$ may be given by[2]

$$\langle S^2\rangle = \lambda^{-2} f_S(\lambda L; \lambda^{-1}\kappa_0, \lambda^{-1}\tau_0) \tag{5}$$

where the function f_S is defined by

$$f_S(L; \kappa_0, \tau_0) = \frac{{\tau_0}^2}{\nu^2} f_{S,KP}(L) + \frac{{\kappa_0}^2}{\nu^2}\left[\frac{L}{3r}\cos\varphi - \frac{1}{r^2}\cos(2\varphi) + \frac{2}{r^3 L}\cos(3\varphi) - \frac{2}{r^4 L^2}\cos(4\varphi) + \frac{2}{r^4 L_2}e^{-2L}\cos(\nu L + 4\varphi)\right] \tag{6}$$

with

$$\nu = ({\kappa_0}^2 + {\tau_0}^2)^{1/2} \tag{7}$$

$$r = (4 + \nu^2)^{1/2} \tag{8}$$

$$\varphi = \cos^{-1}(2/r) \tag{9}$$

and with $f_{S,KP}$ being the function f_S for the KP wormlike chain[2,14] and being given by

$$f_{S,KP} = \frac{L}{6} - \frac{1}{4} + \frac{1}{4L} - \frac{1}{8L^2}(1 - e^{-2L}) \tag{10}$$

In the limit of $\lambda L \to \infty$, we have

$$\lim_{\lambda L\to\infty} f_S(\lambda L)/\lambda L = c_\infty/6 \tag{11}$$

with

$$c_\infty = \frac{4 + (\lambda^{-1}\tau_0)^2}{4 + (\lambda^{-1}\kappa_0)^2 + (\lambda^{-1}\tau_0)^2} \tag{12}$$

If x is the degree of polymerization of a given real chain, then $\langle S^2\rangle/x$ and x are related to f_S and L by the equations

$$\langle S^2\rangle/x = (M_0\lambda^{-1}/M_L)[f_S(\lambda L; \lambda^{-1}\kappa_0, \lambda^{-1}\tau_0)/\lambda L] \tag{13}$$

and

$$\log x = \log(\lambda L) + \log(\lambda^{-1}M_L/M_0) \tag{14}$$

respectively, with M_0 the molecular weight of its repeat unit. From eqs 11 and 13, we have

$$\lim_{x\to\infty}\langle S^2\rangle/x = M_0\lambda^{-1}\, c_\infty/6M_L \tag{15}$$

The ratio $\langle S^2\rangle/x_w$ is plotted against log x_w in Figure 6 with the present data for a-PαMS with $f_r = 0.72$ in cyclohexane at 30.5 °C (Θ) (unfilled circles). For comparison, it also includes the previous data for a-PS with

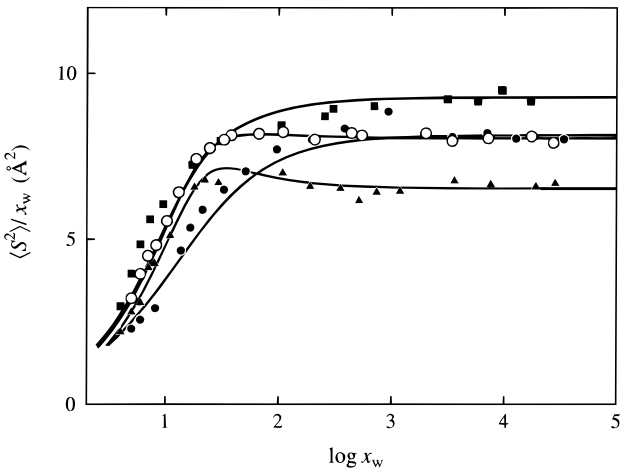

Figure 6. Plots of $\langle S^2\rangle/x_w$ against log x_w: (○) present data for a-PαMS with $f_r = 0.72$ in cyclohexane at 30.5 °C; (●) previous data for a-PS with $f_r = 0.59$ in cyclohexane at 34.5 °C;[22,28] (▲) previous data for a-PMMA with $f_r = 0.79$ in acetonitrile at 44.0 °C;[4,29] (■) previous data for i-PMMA with $f_r \simeq 0.01$ in acetonitrile at 28.0 °C.[26] The solid curves represent the respective best-fit HW theoretical values calculated with the model parameters listed in Table 4.

Table 4. Values of the HW Model Parameters

polymer (f_r)	solvent	temp, °C	$\lambda^{-1}\kappa_0$	$\lambda^{-1}\tau_0$	λ^{-1}, Å	M_L, Å^{-1}
a-PαMS (0.72)	cyclohexane	30.5	3.0	0.9	46.8	39.8
a-PS (0.59)	cyclohexane	34.5	3.0	6.0	20.6	35.8
a-PMMA (0.79)	acetonitrile	44.0	4.0	1.1	57.9	36.3
i-PMMA (0.01)	acetonitrile	28.0	2.5	1.3	38.0	32.5

$f_r = 0.59$ in cyclohexane at 34.5 °C (Θ)[22,28] (filled circles), a-PMMA with $f_r = 0.79$ in acetonitrile at 44.0 °C (Θ)[4,29] (filled triangles), and i-PMMA with $f_r \simeq 0.01$ in acetonitrile at 28.0 °C (Θ)[26] (filled squares). The solid curves represent the respective best-fit HW theoretical values calculated from eqs 5−10 with the values of the model parameters listed in Table 4. The theoretical curve for a-PαMS may reproduce well the experimental values as in the cases of a-PS and a- and i-PMMAs.

It is seen from Figure 6 that a-PαMS and a-PS have almost the same asymptotic values of the ratio $\langle S^2\rangle/x_w$ in the limit of $x_w \to \infty$, which are 8.0_5 Å^2 and 8.1_3 Å^2,[28] respectively, while their behavior is quite different in the oligomer region. The shoulder part of the curve is much more square for a-PαMS than for a-PS, indicating that the former is of stronger helical nature than the latter. The values of the ratio for a-PαMS are nearly equal to those for i-PMMA in the range of $x_w \lesssim 10^2$, while its asymptotic value for the former is smaller than that for the latter, which is 9.3_1 Å^2,[26] indicating also that the former is of stronger helical nature than the latter. Although the curve for a-PαMS is always higher than that for a-PMMA, for which the asymptotic value of the ratio is 6.5_7 Å^2,[29] the two curves are rather similar to each other in shape. Strictly, however, the ratio for the former does not exhibit such a clear maximum as that for the latter does at $M_w \simeq 3 \times 10^3$, indicating that the former is of somewhat weaker helical nature.

The difference in the behavior of the ratio $\langle S^2\rangle/x_w$ mentioned above arises from those in chain stiffness and local chain conformations. It is then important to emphasize again that its asymptotic value cannot be directly correlated to the chain stiffness (λ^{-1}) and that neither the Kuhn statistical segment length nor the persistence length can in general be a measure of chain stiffness, as mentioned in previous papers.[2,4,26]

Table 5. Values of the Characteristic Helix Parameters

polymer (f_r)	solvent	temp, °C	ρ, Å	h, Å
a-PαMS (0.72)	cyclohexane	30.5	$14._3$	$27._0$
a-PS (0.59)	cyclohexane	34.5	1.3_7	$17._3$
a-PMMA (0.79)	acetonitrile	44.0	$13._5$	$23._3$
i-PMMA (0.01)	acetonitrile	28.0	$12._0$	$39._1$

Finally, we note that the value of M_L for a-PαMS is somewhat smaller than the value 45.7 Å^{-1} corresponding to its chain fully extended to the all-trans conformation, as in the cases of a-PS[22,28] and a- and i-PMMAs.[4,26,29]

Local Chain Conformations. Before proceeding to discuss the local chain conformations of a-PαMS in comparison with those of a-PS and a- and i-PMMAs previously studied[2,4,26] on the basis of the obtained values of the HW model parameters κ_0, τ_0, and λ^{-1},[2] we first give a brief re-explanation of the term *helical nature*,[2] as used in the preceding sections. According to the HW chain model, a flexible polymer chain in dilute solution may be pictured as a regular helix (i.e., the characteristic helix) disturbed (or destroyed) by thermal fluctuations or a random coil retaining more or less helical portions. The shape of the characteristic helix may be determined as a space curve by the radius ρ and pitch h, which may be written in terms of κ_0 and τ_0 as

$$\rho = \kappa_0/(\kappa_0^2 + \tau_0^2) \tag{16}$$

$$h = 2\pi\tau_0/(\kappa_0^2 + \tau_0^2) \tag{17}$$

and the degree of disturbance (thermal fluctuation) may be represented by the parameter λ ($=k_BT/2\epsilon$ with k_B the Boltzmann constant, T the absolute temperature, and ϵ the bending force constant), so that the regular helical structure is destroyed to a less extent in the chain with larger stiffness λ^{-1}. In general, the chain of strong helical nature has large ρ (compared to h) and large λ^{-1} and, thus, retains rather large and clearly distinguishable helical portions in dilute solution. Note that the chain with vanishing ρ, i.e., the KP wormlike chain,[2,14] has no helical nature irrespective of the value of λ^{-1} since its characteristic helix becomes a straight line (rod) and that the chain with small λ^{-1} is not of strong helical nature irrespective of the shape of its characteristic helix.

In Table 5 are given the values of ρ and h calculated from eqs 16 and 17 with the values of $\lambda^{-1}\kappa_0$, $\lambda^{-1}\tau_0$, and λ^{-1} given in Table 4 for the a-PαMS chain and also for the a-PS and a- and i-PMMA chains. The values of ρ and h for the a-PαMS chain are nearly equal to those for the a-PMMA chain, indicating that the characteristic helices for both chains are similar to each other in size and shape. However, λ^{-1} is smaller for the former. The characteristic helix for the i-PMMA chain is more extended than that for the a-PαMS chain, and λ^{-1} is smaller for the former. Furthermore, the characteristic helix for the a-PS chain is much more extended (closer to a straight line) than that for the i-PMMA chain, and the former has the smallest value of λ^{-1} of these four polymers. From these observations, it may be concluded that the order of the strength of helical nature of the four polymers is a-PMMA > a-PαMS >i-PMMA > a-PS.

In order to visualize such a difference in local chain conformation (or helical nature) between these polymers, we have generated a HW Monte Carlo chain[2,4]

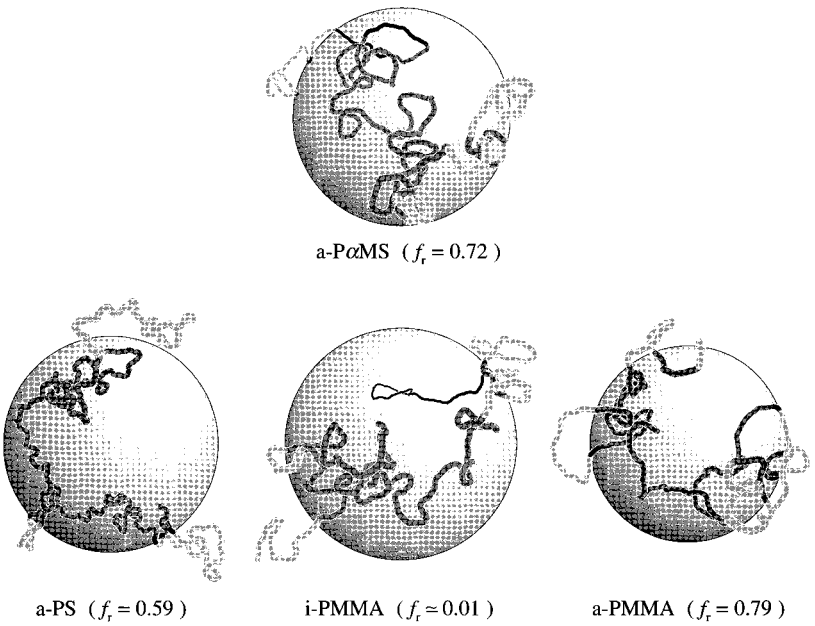

Figure 7. Representative instantaneous contours of HW Monte Carlo chains corresponding to the a-PαMS, a-PS, and i- and a-PMMAs with $x = 500$ such that their radii of gyration S are just equal to their respective $\langle S^2\rangle^{1/2}$ (see the text).

corresponding to the a-PαMS with $x = 500$ to compare it with those corresponding to the a-PS and a- and i-PMMAs previously obtained, each also with $x = 500$.[2,4,26] Note that for this value of x (x_w), their $\langle S^2\rangle/x_w$ values already reach nearly the respective asymptotic ones. The details of the Monte Carlo method are given in section 5.1.3 of ref 2. In Figure 7 are depicted representative instantaneous chain contours obtained here and previously in such a way that their radii of gyration S are just equal to the respective $\langle S^2\rangle^{1/2}$, where the pictures for the a-PS and a- and i-PMMA chains have been arranged from left to right in order of the strength of helical nature, for convenience. The shaded sphere has the radius S, which is equal to 63.6, 63.2, 57.4, and 67.8 Å for a-PαMS, a-PS, a-PMMA, and i-PMMA, respectively, and which is nearly proportional to the asymptotic value of $(\langle S^2\rangle/x_w)^{1/2}$. As seen from the figure, the chain contour of the a-PαMS is rather smooth with the retention of distinguishable helical portions similar to those of the a-PMMA; the latter tends to retain such portions more significantly and take a more compact global conformation. The i-PMMA chain tends to take more extended conformations than the a-PαMS chain. Further, it is interesting to note that the chain contour of the a-PS is much more random than that of the a-PαMS, while these two polymers have almost the same asymptotic value of $\langle S^2\rangle/x_w$, as seen from Figure 6. Such a difference in local chain conformation cannot be clarified on the basis of the Gaussian chain model.

Concluding Remarks

We have determined $\langle S^2\rangle$ for a-PαMS with $f_r = 0.72$ in cyclohexane at 30.5 °C over a wide range of weight-average degree of polymerization x_w, including the oligomer region. From an analysis of the dependence of $\langle S^2\rangle/x_w$ on x_w on the basis of the HW chain model, we have been able to determine the HW model parameters, the results giving valuable information about the local chain conformations of a-PαMS in dilute solution. As was expected from the chemical structure of the a-PαMS chain, as mentioned in the Introduction, it has then been found from the values of the model parameters that the a-PαMS chain tends to retain large and clearly distinguishable helical portions in dilute solution just as the a-PMMA chain,[4] although the helical nature of the former is somewhat weaker than that of the latter. This feature of the a-PαMS chain may be considered to have a significant effect on other equilibrium conformational and steady-state transport properties. We shall continue to study these dilute solution properties of a-PαMS in forthcoming papers.

References and Notes

(1) Konishi, T.; Yoshizaki, T.; Shimada, J.; Yamakawa, H. *Macromolecules* **1989**, *22*, 1921 and succeeding papers.
(2) Yamakawa, H. *Helical Wormlike Chains in Polymer Solutions*; Springer: Berlin, 1997.
(3) Yamakawa, H. *Polym. J.* **1999**, *31*, 109.
(4) Tamai, Y.; Konishi, T.; Einaga, Y.; Fujii, M.; Yamakawa, H. *Macromolecules* **1990**, *23*, 4067.
(5) Yoon, D. Y.; Flory, P. J. *Polymer* **1975**, *16*, 645.
(6) Fujii, M.; Nagasaka, K.; Shimada, J.; Yamakawa, H. *Macromolecules* **1983**, *16*, 1613.
(7) Sundararajan, P. R. *Macromolecules* **1977**, *10*, 623.
(8) Kato, T.; Miyaso, K.; Noda, I.; Fujimoto, T.; Nagasawa, M. *Macromolecules* **1970**, *3*, 777.
(9) Noda, I.; Mizutani, K.; Kato, T.; Fujimoto, T.; Nagasawa, M. *Macromolecules* **1970**, *3*, 787.
(10) Tsunashima, Y. Ph.D. Thesis, Kyoto University, 1972.
(11) Mays, J. W.; Hadjichristidis, N.; Graessley, W. W.; Fetters, L. J. *J. Polym. Sci., Polym. Phys.* **1986**, *24*, 2553.
(12) Li, J.; Harville, S.; Mays, J. W. *Macromolecules* **1997**, *30*, 466.
(13) Yamakawa, H. *Modern Theory of Polymer Solutions*; Harper & Row: New York, 1971.
(14) Kratky, O.; Porod, G. *Recl. Trav. Chim.* **1949**, *68*, 1106.
(15) Osa, M.; Sumida, M.; Yoshizaki, T.; Yamakawa, H.; Ute, K.; Kitayama, T.; Hatada, K. *Polym. J.* **2000**, *32*, 361.
(16) Elgert, K.-F.; Seiler, E. *Makromol. Chem.* **1971**, *145*, 95.
(17) Wicke, R.; Elgert, K.-F. *Makromol. Chem.* **1977**, *178*, 3075.
(18) Deželić, Gj.; Vavra, J. *Croat. Chem. Acta* **1966**, *38*, 35.
(19) Berry, G. C. *J. Chem. Phys.* **1966**, *44*, 4550.
(20) Bawn, C. E. H.; Freeman, R. F. J.; Kamalidin, A. R. *Trans. Faraday Soc.* **1950**, *46*, 862.
(21) Johnson, B. L.; Smith, J. In *Light Scattering from Polymer Solutions*; Huglin, M. B., Ed.; Academic Press: London, 1972; Chapter 2.
(22) Konishi, T.; Yoshizaki, T.; Saito, T.; Einaga, Y.; Yamakawa, H. *Macromolecules* **1990**, *23*, 290.

(23) Kato, T.; Miyaso, K.; Nagasawa, M. *J. Phys. Chem.* **1968**, *72*, 2161.
(24) Cowie, J. M. G.; Bywater, S. *J. Polym. Sci., Part A-2* **1968**, *6*, 499.
(25) Lindner, J. S.; Hadjichristidis, N.; Mays, J. W. *Polym. Commun.* **1989**, *30*, 174.
(26) Kamijo, M.; Sawatari, N.; Konishi, T.; Yoshizaki, T.; Yamakawa, H. *Macromolecules* **1994**, *27*, 5697.
(27) Abe, F.; Einaga, Y.; Yamakawa, H. *Macromolecules* **1994**, *27*, 3262.
(28) Abe, F.; Einaga, Y.; Yoshizaki, T.; Yamakawa, H. *Macromolecules* **1993**, *26*, 1884.
(29) Abe, F.; Horita, K.; Einaga, Y.; Yamakawa, H. *Macromolecules* **1994**, *27*, 725.

MA000353I